PNAS

Supporting Information for
Naturally mutagenic sequence diversity in a human type II topoisomerase

Afif F. Bandak, Tim R. Blower, Karin C. Nitiss, Raveena Gupta, Albert Y. Lau, Ria Guha, John L. Nitiss, and James M. Berger

Dr. James M Berger
Email: jmberger@jhmi.edu

This PDF file includes:

Supplementary methods
Figures S1 to S8
Table S1
Legends for Movies S1 to S2
Legends for Datasets S1 to S2
Legend for Software S1
SI References

Other supporting materials for this manuscript include the following:

Movies S1 to S2
Dataset S1 to S2
Software S1

SUPPLEMENTARY METHODS

Yeast growth

Yeast cells were routinely grown in YPDA media (20g/L dextrose, 20 g/L Bacto peptone, 10 g/L yeast extract, 10 mg/L adenine sulfate. Yeast strains carrying plasmids were grown in synthetic dextrose (SD) media containing 20g/L dextrose, 1.7 g/L yeast nitrogen base without amino acids and ammonium sulfate, 5 g/L ammonium sulfate, amino acids, uracil, and adenine. For solid media, 15g/L Bacto agar was added. Selective media deletes one or more amino acids or nucleobases e.g., SD-Ura lacks uracil and selects for plasmids expressing the yeast *URA3* gene.

Yeast strains

Etoposide sensitivity experiments were carried out in YMM10t2-4 (*ura3-52; his3-Δ200; leu2-Δ1; trp1-Δ63; lys2-801amb; ade2-101oc;Δpdr18::hisG-URA3-hisG;Δpdr12::hisG; Δsnq2::hisG; pdr5::TRP1; Δpdr10::hisG; Δpdr15::loxP-KANMX-loxP;Δyor1::HIS3;Δbat1::HIS3; Δycf1::HIS3 top2-4*) has been previously described (1, 2). Isogenic pairs of *RAD52* and *rad52Δ* cells were JN362a and JN394 (3), and in some cases strains also carried the *top2-4* allele (4).

Expression of hTOP2β in yeast for* in vivo *studies

The plasmid pKN17 was used as a template to generate the PCR products for cloning hTOP2β using standard Gibson assembly protocols (5). PCR products were set up using iProof High-Fidelity PCR kit and the GC buffer (Bio-Rad). Since pKN17 proved to be quite unstable in *E. coli*, a new construct was designed for some of the experiments described here to remove repeated sequences that are present in pKN17 as well as to reverse the orientation of the hTOP2β transcript. To accomplish this, YCplac33 was digested with PvuII in order to remove the MCS and the M13 primer binding sites and the fragment was dephosphorylated. A PCR product containing hTOP2β coding sequence and its 3′ UTR were amplified from pKN17, phosphorylated, and ligated into the PvuII-digested YCplac33. Clones were identified where the bacterial ori was in the same orientation as the transcription of the hTOP2β sequence, resulting in plasmid pKN27. Since we suspected that the human hTOP2β UTR might be sub-optimal for expression in yeast, the 3′ end of hTOP2β including the hTOP2β 3′-UTR was removed by digestion with AleI and SfoI. The plasmid backbone was dephosphorylated and ligated with a fragment (AleI/XhoI blunted) derived from the Gal1-hTOP2β expression vector containing 177 bp of the scTOP2 3′-UTR sequences in order to generate pKN28. The pKN28:K600T plasmid was constructed by digesting hTOP2β-12UraC K600T and ligating the fragment into digested pKN28. The presence of the K600T mutation was confirmed by DNA sequencing.

Construction and screening for etoposide sensitive alleles of hTOP2β

Mutants were generated using a fragment-based approach for performing region-specific mutagenesis and regeneration of a functional hTOP2β in pKN17 without passage through *E. coli*. To make gapped plasmids, the coding sequence of hTOP2β was scanned for presence of restriction enzyme half-sites that would create a new unique restriction site when the two halves were joined. Discrete regions of hTOP2β were specifically chosen where the two halves would leave a gap of 0.75-1.5 kb of coding sequence. The Δ265, Δ438, Δ500, Δ651, and Δ1005 primers that contained enzyme half-sites at the 5' ends were phosphorylated prior to setting up PCR. The same was done for the corresponding reverse primers. High fidelity PCR enzymes (Q5® High-Fidelity 2X Master mix from NEB, iProof High-Fidelity DNA polymerase from Bio-Rad, or Thermo Platinum™ SuperFi™ PCR Master mix from ThermoFisher Scientific) were used in all experiments. PCR reactions were set up according to the manufacturer's protocols. After PCR, the products of the expected sizes were gel isolated, the DNA extracted, ligated, and transformed into *E. coli* strain XL1-Blue. Plasmid DNA was extracted and clones were tested for the presence of the new, unique restriction site. The constructed plasmids and relevant oligonucleotides are summarized in **Table SM1**. Correct clones were linearized and used during the *in vivo* recombination along with mutagenized inserts.

Table SM1: Primers for generating deletion plasmids (restriction enzyme sites and the half-sites are underlined):

Primer name	Sequence (5' to 3')	Upon ligation, the following site was created:
F–hTOP2b-AA265-494-gap–Nru1	CGAGACAGATACGGAGTTTTTCCAC	Nru1 site TCG + CGA = TCGCGA
R–hTOP2b-AA265-494-gap-Nru1	CGAACCAGCCAAATCATATGCCCTT	
R-hTOP2b-AA438-737-gap-Afe1	GCTGAGTCTGAGCCTTAAATTTCAC	Afe1 site ACG + GCT= AGCGCT
F-hTOP2b-AA438-737-gap-Afe1	GCTTTAAACCTGGCCAGCGG	
R-hTOP2b-AA500-723-gap-Pme1	AAACTCCGTATCTGTCTCGTCC	Pme1 site GTTT + AAAC = GTTTAAAC
F-hTOP2b-AA500-723-gap-Pme1	AAACTCAGACAATGAAAGATCTATACC	
F-hTOP2b-AA651-1042-gap-Nru1	CGATTAAGTTATTACGGTTTACG	Nru1 site TCG + CGA = TCGCGA
R-hTOP2b-AA651-1042-gap-Nru1	CGATGCCTTTCCATATCAGC	
F-hTOP2b-AA1005-1312-gap-Pme1	AAACACCTACATCATCTGGTAAACCTAGTG	Pme1 site GTTT + AAAC = GTTTAAAC
R-hTOP2b-AA1005-1312-gap- Pme1	AAACTTTATGCAGTCCAGCAGCTTC	

The GeneMorph II Random Mutagenesis kit (Agilent, part number 200550) was used to introduce mutations in hTOP2β using the primer pairs listed in **Table SM2 (next page)**. The PCR template was the pKN17 plasmid and PCR conditions generating an average of only one mutation per kilobase were used.

Table SM2. Primers for mutagenic PCR.

Primer name	Sequence (5' to 3')	Region covered (AAs)
Beta-S14-nt695	GCATAACATTCCAACCAGATCTGTC	232-552 for use with the Δ265-494 gapped plasmid
Beta-A8-nt1654	TCTTTCCATAGCGTAAGGTTTTCAG	
Beta-S15-nt1396	AACATTCCCTGGAGTGTACACTG	466-768 for use with the Δ500-723 gapped plasmid
Beta-A10-nt2303	CAACAGAGCCAGCCAACTG	
Beta-S16-nt1804	GAACTTTCCTTCTACAGTATTCC	602-1097 for use with the Δ651-1042 gapped plasmid
Beta-A11-nt3291	CCTCTCTGGACTAACATTTG	
Beta-S17	GTTAGAACTTGGACACAGG	944-1351 for use with the Δ1005-1312 gapped plasmid
Beta-A12	CTTGGAATAACCACAGGTTC	

Etoposide hypersensitive mutant screen

The yeast strain YMM10t2-4 was inoculated in YPDA medium and shaken at 25 °C until the OD_{600} between 1.0-2.0 was reached. YMM10t2-4 was co-transformed with 200-400 ng of the mutagenized hTOP2β product and 1.5-2 □g of the gapped plasmid, along with 200 □g sonicated salmon sperm carrier DNA using a standard yeast lithium transformation protocol (6). Yeast were plated to SD-ura plates and grown at 25 °C for approximately 7 days.

All colonies that grew at 25 °C were transferred to fresh SD-ura plates and, following growth, the plates were replica-plated to SD-ura plates containing no drug or 10 $\mu g.ml^{-1}$ etoposide (Sigma) and grown at 34 °C. Patch plates were scored 3-4 days later for complementation and drug sensitivity. Colonies that failed to grow on drug-free SD-ura plates were not analyzed further. Isolates that grew on the drug-free plates but not the plates containing 10 $\mu g.ml^{-1}$ etoposide were streaked for single colonies and the single colonies were assessed for etoposide sensitivity by replica plating to SD-ura media containing 10 $\mu g.ml^{-1}$ etoposide. Cells were retested for etoposide hypersensitivity using a spot test. Briefly, two colonies from each isolate were inoculated into SD-ura media and incubated overnight on a rotator at 34 °C. The following day, the cells were diluted to OD_{600} = 0.3, and 1:5 serial dilutions were made in SD-ura media. Duplicate 3 µl drops of the serial dilutions were spotted onto SD-ura plates containing DMSO, 5 $\mu g.ml^{-1}$ etoposide, or 10 $\mu g.ml^{-1}$ etoposide and the plates were incubated at 34 °C for 3-4 days. The plates were assessed for growth in the presence of etoposide. An example of this confirmatory screen is shown in **Figure S1B**.

Etoposide-sensitive clones were further tested using a yeast clonogenic survival assay. Briefly, candidate clones were inoculated into SD-ura media and incubated overnight in a rotator at 34 °C. The following day, cells were diluted to 2 x 10^6 $cells.ml^{-1}$ and aliquots were exposed to varying concentrations of etoposide for 24 hours at 34 °C. Serial dilutions were made and cells plates to SD-ura at 34 °C for 3-5 days. The colonies were counted and the results were calculated based on the survival of the cells compared to the viable count at the time of drug addition, *t*=0.

Yeast clones that were hypersensitive to etoposide were treated with zymolase (Seikagaku) and the region containing the mutagenized sequences was PCR amplified using the primers shown in **Table SM3**. The resulting PCR products were subjected to Sanger sequencing.

Table SM3. PCR primers for mutant fragment recovery from etoposide hypersensitive isolates.

Mutated region	Primer name	Primer sequence (5'-3')
Δ265-494	Beta-S2	CCAGTAGTAGAACACAAGGTAG
	R-hTOP2b-AA651-1042-gap-Nru1	CGATGCCTTTCCATATCAGC
Mutated region	Primer name	Primer sequence (5'-3')
Δ500-723	Beta-S4	TACAAAAGGTGGACGGCAC
	Beta-A4	CTGTGTTTCTGTCCACTAC
Δ651-1042	Beta-S6	CTGAAAACCTTACGCTATGG
	Beta-A2	CTGAATCGGAGGAACTATC
Δ1005-1312	Beta-S8	TCTGTTGCTGAGATGTCG
	Beta-A12	CTTGGAATAACCACAGGTTC

Assessment of rad52- dependent lethality

Isogenic yeast strains that were either repair proficient or repair deficient were inoculated into YPDA and shaken at 25°C (*top2-4*) or 30°C (*TOP2*$^{+}$) overnight. Equal OD units of the yeast strains JN362a, JN394 (isogenic to JN362a but rad52Δ::LEU2), JN362a$_{t2\text{-}4}$, and JN394$_{t2\text{-}4}$ as indicated were transformed with 100 ng plasmid DNA containing various Top2β alleles along with 200 □g carrier DNA using a standard yeast lithium transformation protocol. Equal volumes of the transformations were plated to SD-ura plates. JN362a and JN394 transformations were incubated at 30°C. The JN362a$_{t2\text{-}4}$, and JN394$_{t2\text{-}4}$ transformants were incubated at 25°C and 34°C. Plates were scored for colony formation after 3 days incubation.

Topoisomerase II cloning for protein expression, expression and purification

PCR-amplified full-length topoisomerase genes were inserted by LIC (ligation-independent cloning (7)) into 12UraB (Addgene #48304), a modified version of pRS426 (8). The resulting plasmid (hTOP2β-12UraC) contained galactose-inducible fusions with an N-terminal tobacco etch virus (TEV) protease-cleavable hexahistidine tag. Mutant hTOP2β constructs were generated by site-directed mutagenesis of the hTOP2β-12UraC construct (primers shown in **Table SM4**).

Table SM4. Primers used to generate mutant expression constructs.

Name	Primer
hTOP2β 12UraC K600T_F	CATTACTCCTATTGTAACGGCAAGCAAAAATAAGC
hTOP2β 12UraC K600T_R	GCTTATTTTTGCTTGCCGTTACAATAGGAGTAATG
hTOP2β 12UraC K646E_F	CAGCTAAAGAAGCAGAGGAATATTTTGCTG
hTOP2β 12UraC K646E_R	CAGCAAAATATTCCTCTGCTTCTTTAGCTG
hTOP2β 12UraC S396F_F	GAAAATCCAACTTTTGATTTTCAGACTAAGGAAAACATG
hTOP2β 12UraC S396F_R	CATGTTTTCCTTAGTCTGAAAATCAAAAGTTGGATTTTC
hTOP2β 12UraC S396F_F	TTTTCAATAAGGCAATTAATAAAAACCC
hTOP2β 12UraC K461R_F	GTATTCCCAGACTGGATGAT
hTOP2β 12UraC K461R_R	CTTTGATTTTACTGTATTTTACTGA
hTOP2β 12UraC K631Q_F	GAAAATACAGTACTATAAAGGATTGG
hTOP2β 12UraC K631Q_R	CAGGCTTTCTGGTTTTCTATATGTT
hTOP2β 12UraC R757W_F	GTTTCAAGTGGAATGATAAACGTGA
hTOP2β 12UraC R757W_R	AGGTAAATAAAACTTTCCGCTGG
hTOP2β 12UraC D759G_F	CAAGAGGAATGGTAAACGTGAAGTAAAAGTTG
hTOP2β 12UraC D759G_R	CTTCACGTTTACCATTCCTCTTGAAACAGG
hTOP2β 12UraC K646N_F	CTAAAGAAGCAAACGAATATTTTGCTG
hTOP2β 12UraC K646N_R	CTGTACTAGTACCCAATCCTTTATAG
hTOP2β 12UraC V111I_F	GAAATTTTGATTAATGCTGCTGA
hTOP2β 12UraC V111I_R	ATCAAAGATCTTGTATAAACCTG
hTOP2β 12UraC R761C_F	GAATGATAAATGTGAAGTAAAAGTT
hTOP2β 12UraC R761C_R	CTCTTGAAACAGGTAAATAAAACTTT

Overexpression of the wildtype and mutant constructs was performed in *S. cerevisiae* strain BCY123, with starter cultures grown in complete supplement mixture dropout medium lacking uracil (CSM-URA), supplemented with 2% (vol.vol^{-1}) lactic acid and 1.5% (vol.vol^{-1}) glycerol as carbon sources. CSM-URA starter cultures were then transferred to large YP expression cultures supplemented with 2% (vol.vol^{-1}) lactic acid and 1.5% (vol.vol^{-1}) glycerol (100mL starter with 1L media) and grown at 30 °C, 160 rpm, to an OD_{600} of 0.8-1.0 and induced by the addition of 20 g.l^{-1} galactose. After a further 6 hours growth at 30 °C, 160 rpm, cells were harvested by centrifugation (4,500 x g, 15 min, 4 °C) then re-suspended in lysis buffer (250 mM NaCl, 1 mM EDTA), and frozen drop-wise in liquid nitrogen.

Frozen cells were cryogenically lysed using a Spex 6870 freezer mill, with 15 cycles of 1 min grinding followed by 1 min of cooling. The resulting powder was thawed in A300 (20 mM Tris-HCl [pH 8.5], 300 mM KCl, 20 mM imidazole pH 8.0, 10% [vol.vol^{-1}] glycerol with protease inhibitors [1 µg.ml^{-1} pepstatin A, 1 µg.ml^{-1} leupeptin and 1 mM PMSF]) and clarified by centrifugation (17,000 x g, 20 min, 4 °C). The lysate supernatant was passed over an A300-equilibrated HisTrap HP column (GE Healthcare) using a peristaltic pump and washed with 30 ml of A300 and 25 ml of A100 (20 mM Tris-HCl [pH 8.5], 100 mM KCl, 20 mM imidazole pH 8.0, 10% [vol.vol^{-1}] glycerol with protease inhibitors). The HisTrap HP column was then connected to an Akta Explorer FPLC (GE Healthcare) and linked upstream of a HiTrap S HP column (GE Healthcare) and equilibrated with a further 5 ml of A100. The tandemly coupled columns were next washed with 25 ml B100 (20 mM Tris-HCl [pH 8.5], 100 mM KCl, 200 mM imidazole pH 8.0, 10% [vol.vol^{-1}] glycerol with protease inhibitors) to elute the tagged protein onto the S column, followed by an additional 15 ml of A100 to reduce

imidazole levels. A gradient was then applied to the coupled columns, reaching 100% buffer C (20 mM Tris-HCl [pH 8.5], 500 mM KCl, 10% [vol.vol^{-1}] glycerol with protease inhibitors) over 25 min. Peak fractions were assessed by SDS-PAGE, collected, and concentrated in Amicon 100-kDa-cutoff concentrators (Millipore). His-tagged TEV protease (QB3 MacroLab) was next added to the concentrated samples and incubated at 4 °C overnight. This mixture was then passed over a second HisTrap HP column equilibrated and washed with buffer D (20 mM Tris-HCl [pH 8.5], 500 mM KCl, 20 mM imidazole pH 8.0, 10% [vol.vol^{-1}] glycerol) to remove any uncleaved enzyme and the protease. The flowthrough was collected and concentrated, then separated by gel filtration using an S400 column (GE Healthcare) equilibrated in sizing buffer (20 mM Tris-HCl [pH 7.9], 500 mM KCl, 10% [vol.vol^{-1}] glycerol). Peak fractions were pooled and concentrated by centrifugation at 4000 RPM using a 30-kDa MWCO filter (Amicon). These final purified samples were then combined with a one-third volume of storage buffer (20 mM Tris-HCl [pH 7.9], 500 mM KCl, 70% [vol.vol^{-1}] glycerol), quantified for protein concentration by NanoDrop (ThermoScientific), and were snap frozen as aliquots for storage at -80 °C.

Molecular dynamics simulations

The hTOP2β-DNA-ATP ternary complex model was built using iTASSER (9) based on previous structures of full length scTOP2 (PDB: 4GFH) and the hTOP2β nucleolytic core (PDB: 3QX3). Crystallographic waters were retained and the complex, which contained a total of 39,958 atoms, was solvated with 425,241 atoms water molecules and neutralized by adding sodium and chloride ions to the bulk solution until the salt concentration was 150 mM NaCl. Periodic boundary conditions were imposed on an orthorhombic cell with approximate dimensions 120 Å × 100 Å × 80 Å. The fully solvated system, which contained a total of 465,199 atoms. Periodic boundary conditions were imposed on an orthorhombic unit cell of approximate dimensions 128 Å × 128 Å × 96 Å. The system was energy minimized and equilibrated using constant pressure and temperature (NPT) conditions at 1 atm and 300 K with a timestep of 2 fs. The all-atom potential energy function PARAM27 for proteins and nucleic acids (10) and the TIP3P potential energy function for water (11) were used. Electrostatic interactions were computed using the particle mesh Ewald (PME) algorithm and short-range, non-bonded interactions were truncated to 12 Å. The initial protein configuration was equilibrated for 200 ns in preparation for long timescale simulations. The pre-production and equilibration runs were performed using NAMD 2.9 (12)

Network analysis

MD simulation trajectories were used to construct a dynamic network model (13). In the hTOP2β-DNA-ATP ternary complex, individual amino acid and nucleotides residues define the set of nodes comprising the complex. Edges indicate physical contacts between sequentially non-consecutive nodes, where the threshold for contact is met if a pair of heavy atoms between two nodes reside within 4.5 Å of each other over at least 75% of the MD trajectory. Community structure is identified using the Girvan-Newman algorithm (14).

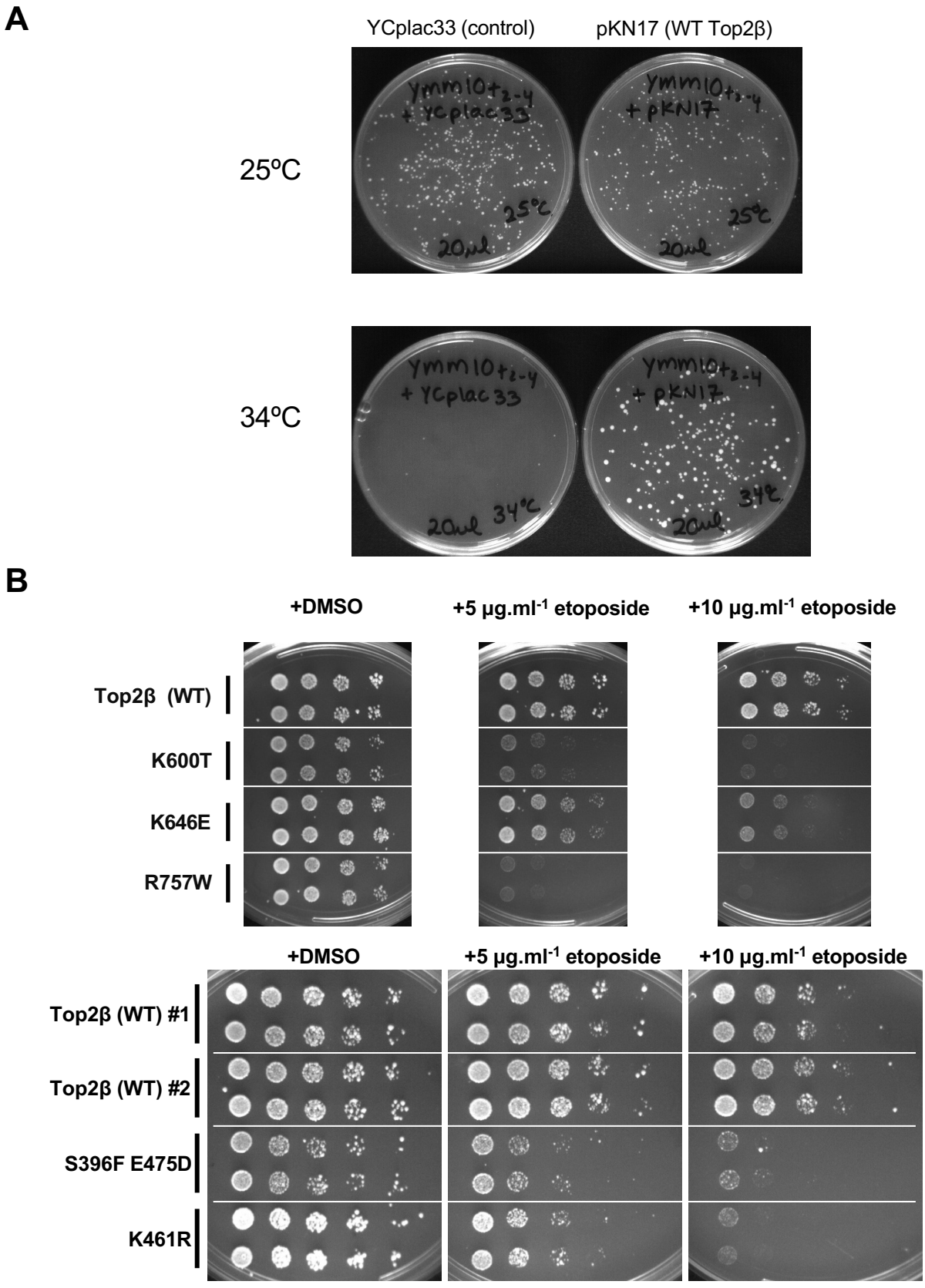

Fig. S1. Selection of Etop^{HS} hTOP2β mutants. **A.** pKN17 complements a top2-4 deficiency. pKN17 (TPI promoter with wild type hTOP2β) or the empty vector YCplac33 were introducing into *TOP2*$^{+}$ or *top2-4* strains. Growth at 34°C was observed when cells were transformed into the *top2-4* strain, while the empty vector did not support growth at 34°C. **B.** After the initial replica plating screen, selected isolates were grown in yeast synthetic media lacking uracil. Cultures were adjusted to an OD600 = 0.3, five-fold serial dilutions were carried out, and 3 µl of the diluted cultures were spotted onto plates containing DMSO, 5 µg.ml^{-1} etoposide, or 10 µg.ml^{-1} etoposide. Plates were incubated at 34 °C for three days. Plates were then photographed by conventional photography. Isolates shown in this figure were the original isolates obtained in the screen that were selected for further study. Results with other isolates are summarized in Table S1, which shows etoposide sensitivity of the original isolates determined by clonogenic survival.

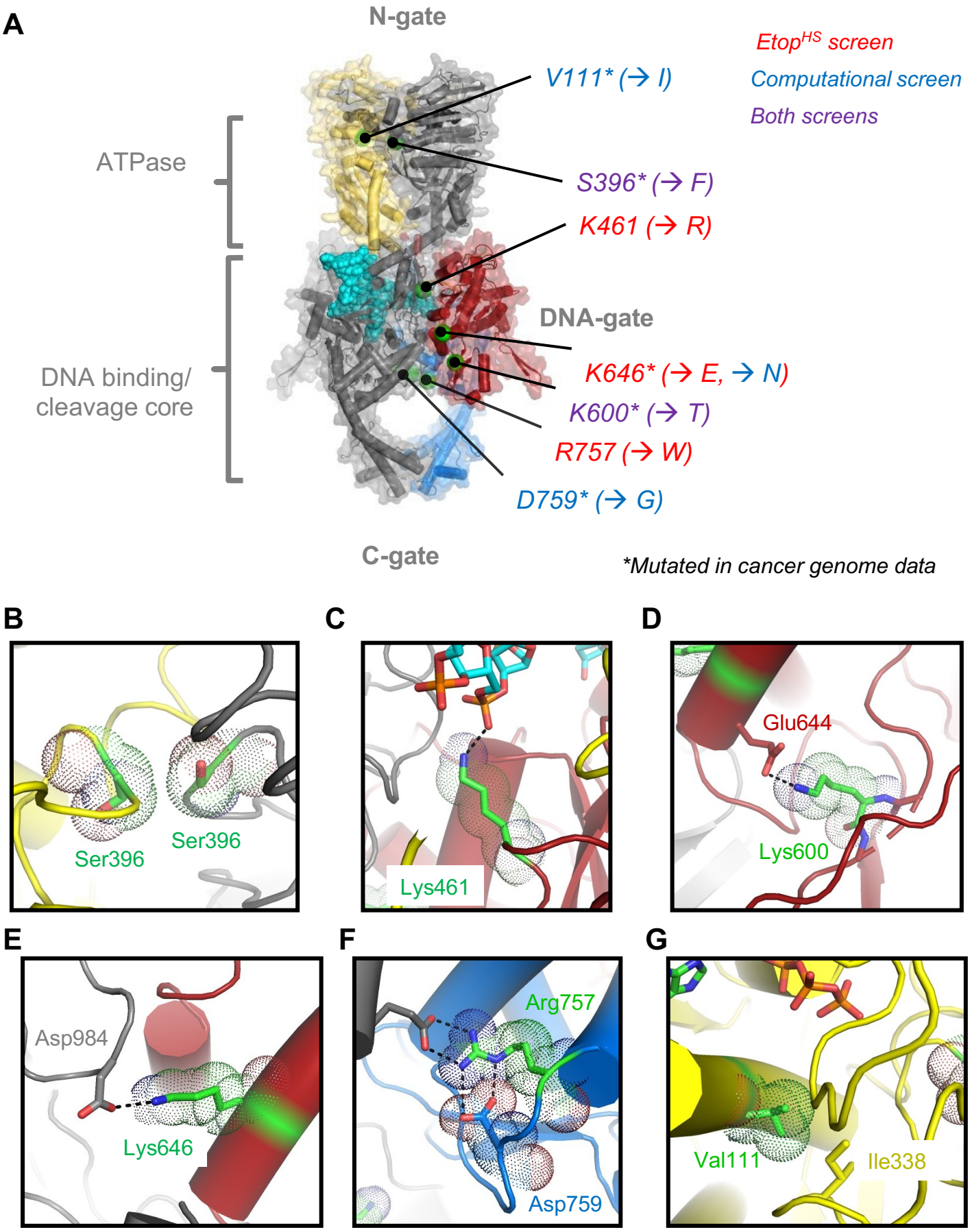

Fig. S2. Schematic of hTOP2β Etop^{HS} and cancer genome mutations studied here and their positions/interactions. (A) Cartoon diagram (overlayed with a transparent surface rendering) of an hTOP2β•DNA•AMPPNP homology model (PDB 4GFH, 3QX3 used as a template) with mutational positions noted by green spheres and labels (label color indicates whether the mutation was identified from the Etop^{HS} screen, the computational screen, or both; an asterisk indicates that this position has a mutation in the cancer genome data (all mutations are indicated by '→' followed by the single letter code for the substitution). The three dimerization interfaces of the protein are denoted (N-gate, DNA-gate, C-gate), as are the catalytic elements of the protein (ATPase, DNA binding/cleavage core). (B- G) Close-up views of the amino acid positions found to be mutated in the EtopHS screen or highlighted by the computational screen and their interacting partners.

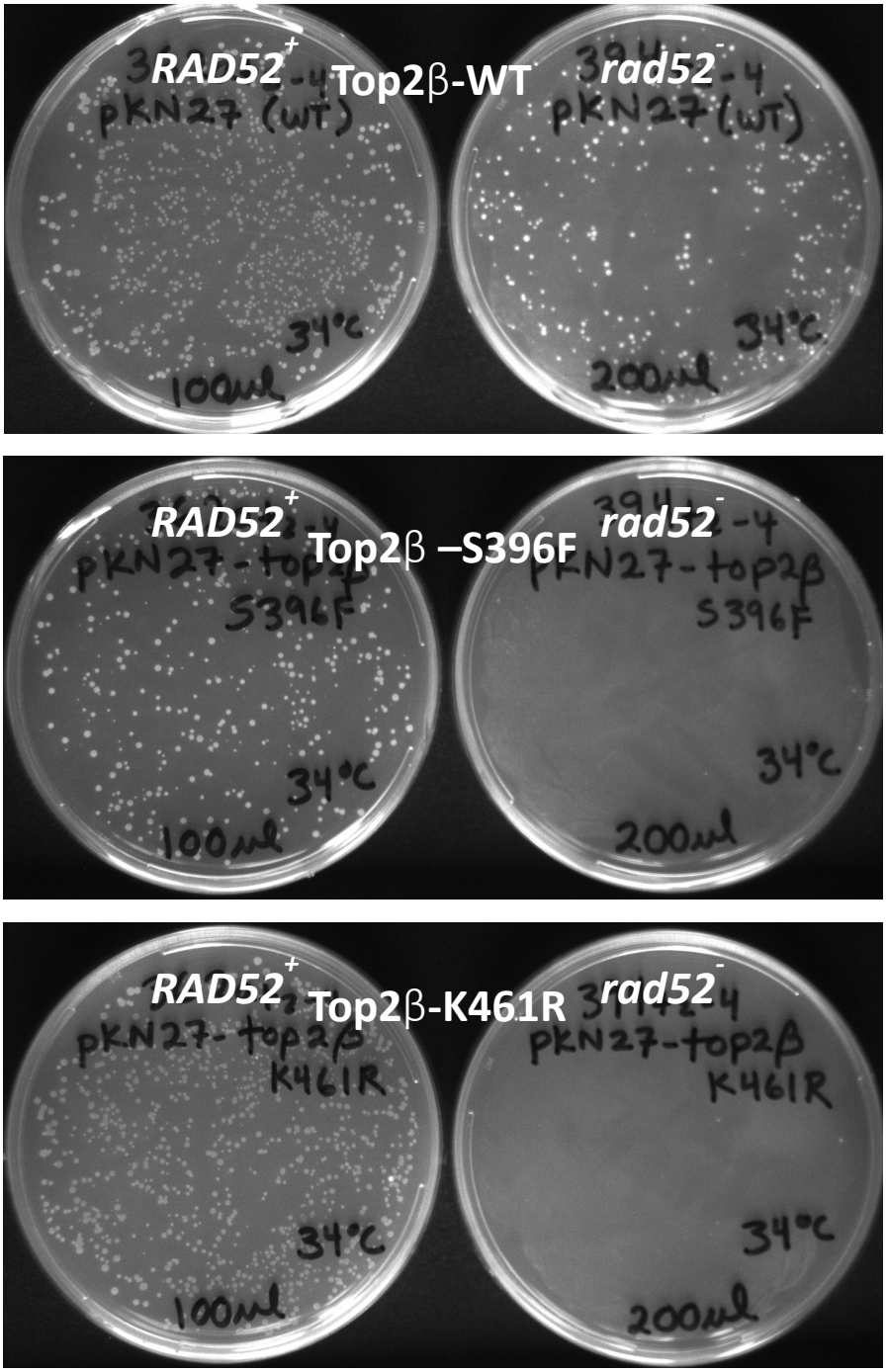

Fig. S3. Expression of hTOP2β$_{S396F}$ and hTOP2β$_{K461R}$ are not viable in rad52-deficient yeast strains. Plasmids expressing hTOP2β$_{WT}$, hTOP2β$_{S396F}$, or hTOP2β$_{K461R}$ were introduced into either RAD52+ or rad52- yeast cells . In the experiment shown , both RAD 52+ or rad52- strains were also top2-4 and cells were incubated for three days at 34°C prior to conventional photography. Note that hTOP2β$_{S396F}$ and hTOP2β$_{K461R}$ allow growth in a RAD52+ strain and therefore encode a functional TOP2 allele.

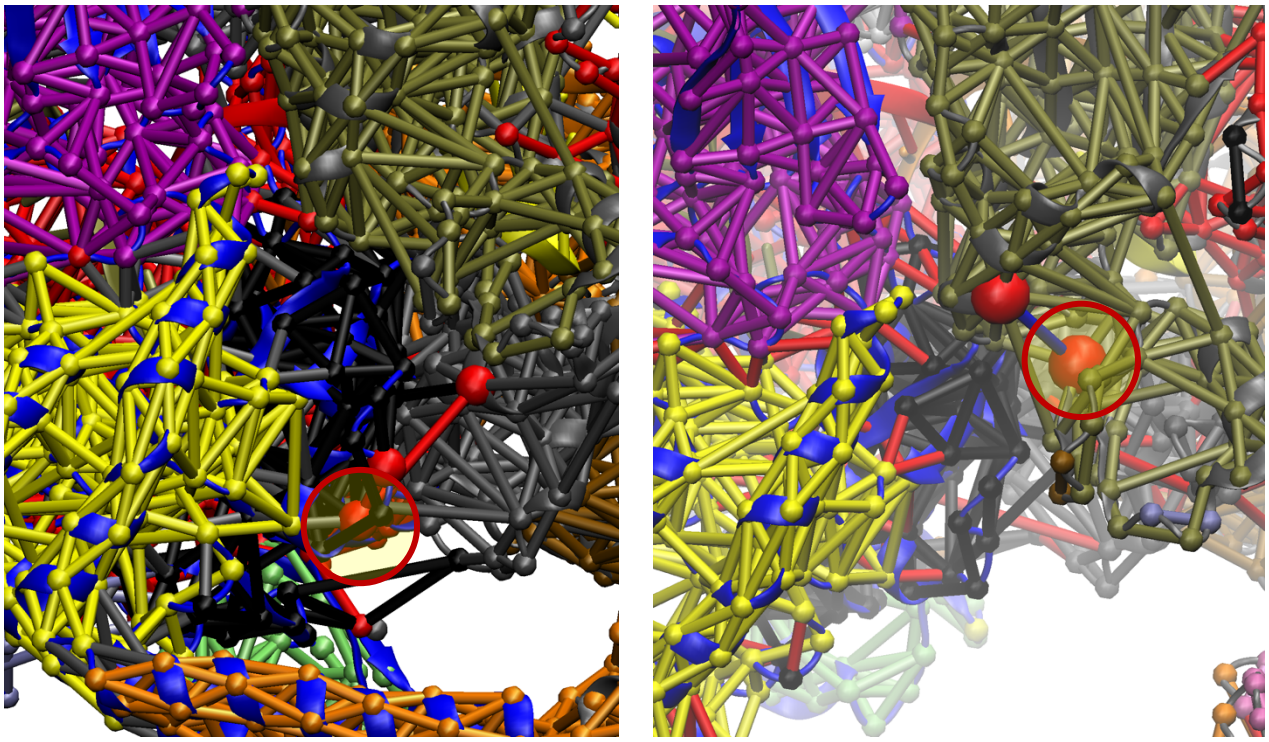

Fig. S4. Network model close-up views for Arg757 and Lys600. Proximal critical node interactions highlighted as red edges for Arg757. The TOPRIM and Greek key structural elements are classified as a single community bridged by an electrostatic interaction between Lys600 and Glu644 (blue edge)

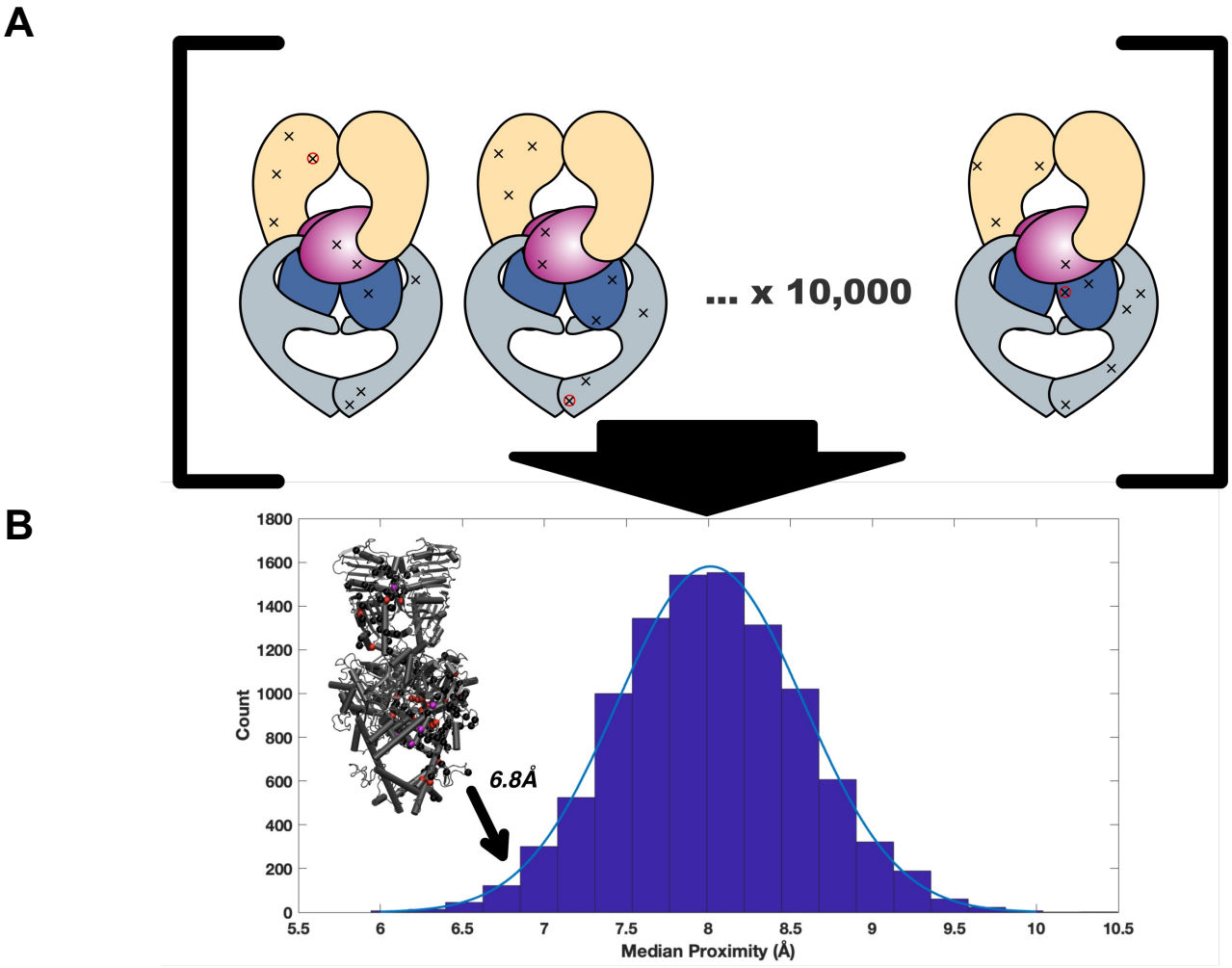

Fig. S5. Analysis of the median proximity between cancer genome database mutations in the human TOP2B gene and critical node residues. (A) Schematic depicting how Monte Carlo simulations were used to generate random sets of mutations throughout the catalytic core of hTOP2β sequence. For each mutation site, an array of distances relative to every critical node reside identified from MD-DNA was measured with the shortest distance recorded in a separate array containing each mutation's proximity to the nearest critical node. 10,000 different simulations were run, with median critical node proximities for the set computed in each iteration. (B) Histogram of median proximities of simulated mutation sets to critical nodes. Mutations present in cancer genome data tend to fall closer to critical nodes (arrow) than expected from random chance.

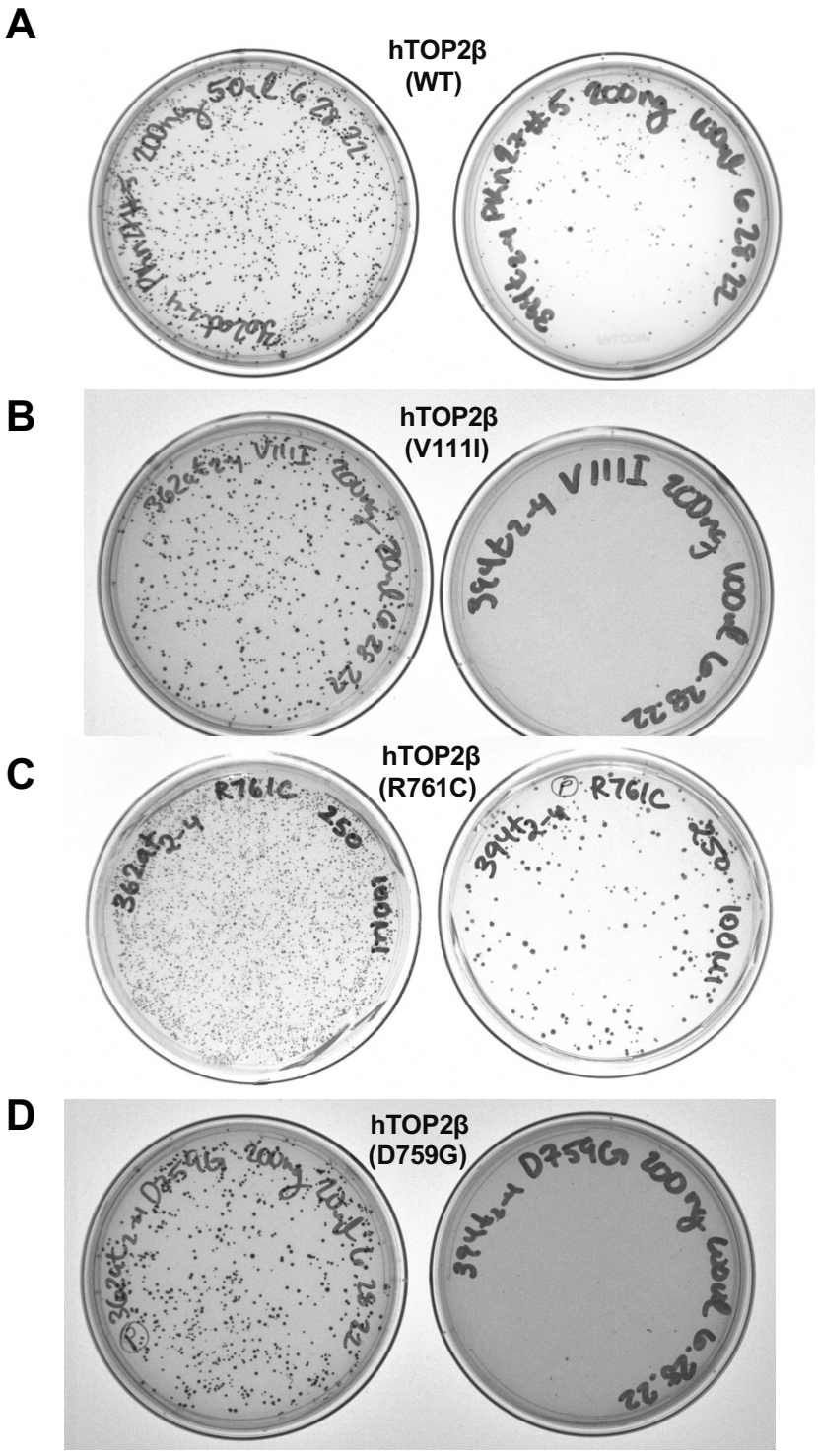

Fig. S6. Expression of hTOP2β$_{V111I}$ and hTOP2β$_{D759G}$ are not viable in *rad52*-deficient yeast strains. Plasmids expressing hTOP2β$_{WT}$, hTOP2β$_{V111I}$, hTOP2β$_{D759G}$, or hTOP2β$_{D761C}$ were introduced into either *RAD52*$^{+}$ or *rad52*$^{-}$ yeast cells. In the experiment shown, both *RAD52*$^{+}$ or *rad52*$^{-}$ strains were also *top2-4* and cells were incubated for three days at 34°C prior to conventional photography. Note that hTOP2β$_{V111I}$,hTOP2β$_{D759G}$ and hTOP2β$_{D761C}$ allow growth in a *RAD52*$^{+}$ strain and therefore encode a functional *TOP2* allele. Only the hTOP2β$_{WT}$ and hTOP 2β$_{D761C}$ alleles conferred growth in the *rad52*$^{-}$ yeast cells.

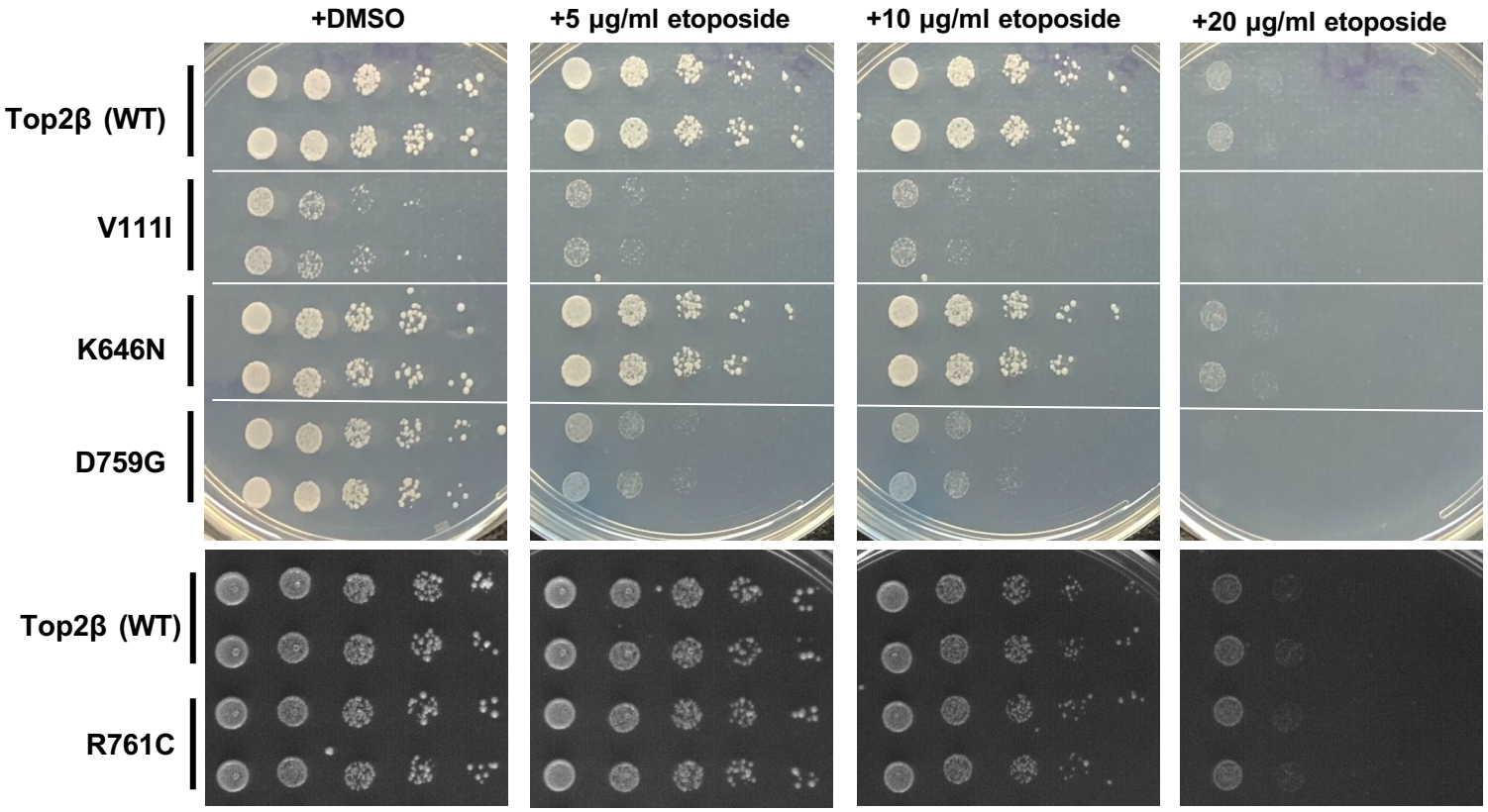

Fig. S7. Etoposide sensitivity testing for cancer mutant dataset mutations. hTOP2β$_{V111I}$ and hTOP2β$_{D759G}$ show significant sensitivity to etoposide, while hTOP2β$_{R761C}$ exhibited sensitivity that was similar to cells expressing wild type Top2β. Experimental conditions were the same as shown in Fig. S1B.

Table S1. Etoposide hyper-sensitive mutants of hTOP2β. Complete data with reconstructed alleles are shown in Figure 1A. Isolates with more than two amino acid substitutions are not listed.

Mutation	No drug, 24 h growth (T=0, 100)	Relative Survival after 10 μg.ml^{-1} etoposide, 24 h	Relative Survival after 20 μg.ml^{-1} etoposide, 24 h
Wildtype pKN17	857	290	162
M277I (ATG→ATA)*	52	32	14
S396F (TCT→TTT)* / ***E475D (GAG→GAT)***	168	48	8
K363N (AAG→AAT)	ND	ND	ND
K461R (AAA→AGA)*	407	22	2.7
V486E (GTG→GAG) / ***R494R (CGA→CGC)***	1360	134	37
G498R (GGA→AGA)	616	21	5
K600T (AAG→ACG)*	765	40	4.7
K632N (AAG→AAT) / ***L658V (TTGGTG)***	589	132	9
K632Q (AAG→CAG)	1149	22	2
K646E (AAG→GAG)*	387	14	1.4
R757W (AGG→TGG)*	439	6.1	0.4
E1078K (GAG→AAG)	601	87	32
R1101K (AGA→AGG)	450	90	15

***Poor growth without drug indicates poor complementation of the *top2-4* allele.**
**** Mutants selected for further study.**
ND – Not analyzed further due to limited sensitivity on preliminary tests.

Movie S1. MD simulation trajectory for hTOP2β•ATP•DNA complex (500 ns).

Movie S2. Full view of community representation for hTOP2β•ATP•DNA complex shown in Fig. 4.

Dataset S1. Raw gel electrophoresis images for Figs. S3, S4, S8

Dataset S2. hTOP2β cancer genome mutation dataset.

Software S1. Script used to perform statistical analysis shown in Fig. S5.

SI REFERENCES

1. J. Anand, Y. Sun, Y. Zhao, K. C. Nitiss, J. L. Nitiss, "Detection of Topoisomerase Covalent Complexes in Eukaryotic Cells" in (2018), pp. 283–299.
2. N. Stantial, *et al.*, Trapped topoisomerase II initiates formation of de novo duplications via the nonhomologous end-joining pathway in yeast. *Proceedings of the National Academy of Sciences* **117**, 26876–26884 (2020).
3. J. Nitiss, J. C. Wang, DNA topoisomerase-targeting antitumor drugs can be studied in yeast. *Proceedings of the National Academy of Sciences* **85**, 7501–7505 (1988).
4. W. Thomas, R. M. Spell, M. E. Ming, C. Holm, Genetic analysis of the gyrase A-like domain of DNA topoisomerase II of Saccharomyces cerevisiae. *Genetics* **128**, 703–716 (1991).
5. D. G. Gibson, *et al.*, Enzymatic assembly of DNA molecules up to several hundred kilobases. *Nat Methods* **6**, 343–345 (2009).
6. R. D. Gietz, R. H. Schiestl, Large-scale high-efficiency yeast transformation using the LiAc/SS carrier DNA/PEG method. *Nat Protoc* **2**, 38–41 (2007).
7. C. Aslanidis, P. J. de Jong, Ligation-independent cloning of PCR products (LIC-PCR). *Nucleic Acids Res* **18**, 6069–74 (1990).
8. T. W. Christianson, R. S. Sikorski, M. Dante, J. H. Shero, P. Hieter, Multifunctional yeast high-copy-number shuttle vectors. *Gene* **110**, 119–122 (1992).
9. Y. Zhang, I-TASSER server for protein 3D structure prediction. *BMC Bioinformatics* **9**, 40 (2008).
10. A. D. MacKerell, *et al.*, All-Atom Empirical Potential for Molecular Modeling and Dynamics Studies of Proteins. *J Phys Chem B* **102**, 3586–3616 (1998).
11. W. L. Jorgensen, J. Chandrasekhar, J. D. Madura, R. W. Impey, M. L. Klein, Comparison of simple potential functions for simulating liquid water. *J Chem Phys* **79**, 926–935 (1983).
12. J. C. Phillips, *et al.*, Scalable molecular dynamics with NAMD. *J Comput Chem* **26**, 1781–1802 (2005).
13. A. Sethi, J. Eargle, A. A. Black, Z. Luthey-Schulten, Dynamical networks in tRNA:protein complexes. *Proceedings of the National Academy of Sciences* **106**, 6620–6625 (2009).
14. M. Girvan, M. E. J. Newman, Community structure in social and biological networks. *Proceedings of the National Academy of Sciences* **99**, 7821–7826 (2002).